Environment and Natural Resources Journal
Volume 22
Issue 5
2024

Warming Effect from Soil Greenhouse Gas Emission of Each Mangrove Zone during the Dry Season in Ngurah Rai Forest Park, Bali, Indonesia

I Putu Sugiana[1*], Tri Prartono[2], Rastina[2], and Alan Frendy Koropitan[2]

[1]*Graduate Program of Marine Science, School of Graduates, IPB University, IPB Dramaga Campus, Bogor 16680, West Java, Indonesia*
[2]*Department of Marine Science and Technology, Faculty of Fisheries and Marine Science, IPB University, IPB Dramaga Campus, Bogor 16680, West Java, Indonesia*

ARTICLE INFO

Received: 5 Feb 2024
Received in revised: 31 Jul 2024
Accepted: 8 Aug 2024
Published online: 22 Aug 2024
DOI: 10.32526/ennrj/22/20240029

Keywords:
Closed-chamber technique/ CO_2/ CH_4/ N_2O/ Mangrove zones/ GHG flux variations

*** Corresponding author:**
E-mail: iptsugiana@apps.ipb.ac.id

ABSTRACT

In addition to functioning as a carbon sink, mangrove soil also releases greenhouse gases (GHGs) through microbial metabolism. GHG flux fluctuates according to the ecological parameters of mangroves and climate variability. We quantified GHG fluxes from the soil using a closed-chamber technique and assessed soil and porewater conditions in three primary mangrove zones (each zone was dominated by one of the mangrove types) at Ngurah Rai Forest Park, Bali, Indonesia, categorized by genera: *Bruguiera*, *Rhizophora*, and *Sonneratia*. We found that the CO_2 flux ranged from 322.5 to 3,494.5 µg/m^2/h, CH_4 flux ranged from -24.7 to 60.9 µg/m^2/h, and N_2O flux ranged from -1.2 to 2.3 µg/m^2/h. None of the GHG fluxes varied significantly between mangrove zones. Overall, the highest CO_2 fluxes were observed in the *Bruguiera* zones, while the highest CH_4 and N_2O fluxes were found in the *Sonneratia* and *Rhizophora* zones, respectively. A significant relationship between GHG fluxes and soil properties, including soil organic carbon (SOC), total Kjeldahl nitrogen (TKN), water content, bulk density, and soil type. The average warming effect on GHG fluxes ranged from 0.9 and 1.8 MgCO_2/ha/year, accounting for only 1.1% to 2.2% of the annual plant carbon sequestration rate of 75.9 to 81.6 MgCO_2/ha/year. These findings suggest that the variability of GHG fluxes is not significantly influenced by mangrove type; instead, soil conditions play a crucial role. Calculations of the net carbon stock may overlook the relatively low warming effect of GHG fluxes in this area.

1. INTRODUCTION

Global warming is the phenomenon of the Earth's average atmospheric temperature increasing due to the presence of greenhouse gases (GHGs) such as carbon dioxide (CO_2), methane (CH_4), and nitrous oxide (N_2O) (Montzka et al., 2011; Kweku et al., 2018). The IPCC report (2021) states that atmospheric CO_2 concentrations have reached 409.9 parts per million (ppm) since the pre-industrial era in 1750. Additionally, the report indicates that CH_4 and N_2O have increased by 5-10 parts per billion (ppb) and one ppb each year, respectively (Reay et al., 2018). Despite their lower concentrations compared to CO_2, CH_4, and N_2O have a global warming potential of 29.8 and 273 times greater than CO_2 over a 100 year period (IPCC, 2021). Hence, their influence must not be overlooked when calculating the atmosphere's Global Warming Potential (GWP).

In addition to serving as a carbon sink in the form of CO_2 absorption, mangrove forests also release GHG fluxes (Alongi, 2014; Chen et al., 2016). Indonesia has the highest proportion of mangrove forests worldwide, accounting for about 19.5% (Bunting et al., 2018). These forests have a carbon uptake rate of 1,190,814 tonsC/ha/year. Nevertheless, GHG emissions are notably substantial, particularly in

Citation: Sugiana IP, Prartono T, Rastina, Koropitan AF. Warming effect from soil greenhouse gas emission of each mangrove zone during the dry season in Ngurah Rai Forest Park, Bali, Indonesia. Environ. Nat. Resour. J. 2024;22(5):449-463. (https://doi.org/10.32526/ennrj/22/20240029)

mangrove forests impacted by pollution, including organic matter (Das et al., 2022). The decomposition of organic matter results in the production of carbon dioxide (CO_2) in the oxic/aerobic soil layer and methane (CH_4) in the anoxic/anaerobic soil layer (Wang et al., 2009; Treat et al., 2015). In addition, N_2O is produced through denitrification processes that utilize NO_3^- (nitrate) or NO_2^- (nitrite) nutrients derived from the nitrification process of NH_4^+ (ammonia). These processes are typically found in mangrove forests with high soil carbon and nitrogen content and low oxygen conditions (Zhu et al., 2013; Queiroz et al., 2019). Hence, accurate data regarding GHG fluxes is necessary to accurately determine the net carbon stock of the mangrove ecosystem.

Variations in environmental condition, such as water salinity, soil type, and soil carbon accumulation capability, are responsible for the differences observed in mangrove vegetation types (Ewel et al., 1998; Srikanth et al., 2016; Raganas and Magcale-Macandog, 2020). The arrangement of mangrove trees differs depending on the dominant species, affecting the amount of organic matter that is contributed to the surrounding environment (Prasad et al., 2010; Mulya and Arlen, 2018). This, in turn, impacts greenhouse gas fluxes and the extent of the warming effect in terms of CO_2-equivalent (Chen et al., 2016; Xu et al., 2021). Various studies have shown that comparing the warming effect caused by GHG emissions with the annual carbon sequestration rate varies across different zones. For instance, the warming effect value of GHG flux in *Kandelia candel* dominated mangrove area is 20.5% (Chen et al., 2016), while it is 24% for CH_4 in *Kandelia obovata* zone (Liu et al., 2020). In the mixed zone consisting of *K. obovata*, *Avicennia marina*, and *Aegiceras corniculatum*, the warming effect of CH_4 is only 4.6% (Zhu et al., 2013). These findings highlight the significant impact of mangrove zoning factors on the warming effect of soil GHG fluxes.

The mangrove ecosystem at Ngurah Rai Forest Park (TAHURA) is the largest mangrove area in Bali, Indonesia. The zonation patterns of mangrove species are evident, with the dominant zones occupied by the genera *Rhizophora*, *Sonneratia*, and *Bruguiera* (Sugiana et al., 2022). The environmental conditions also vary, regarding to salinity, pH, oxidation-reduction potential (ORP), and substrate type (Prinasti et al., 2020; Dewi et al., 2021; Sugiana et al., 2021). These parameters are key factors that control the greenhouse gas flux from mangrove soil (Chen et al., 2016; Kitpakornsanti et al., 2022). Previous research measured GHG flux during the rainy season (Sugiana et al., 2023). However, due to the potential variations that may occur due to seasonal factors (Padhy et al., 2020; Cameron et al., 2021), measurements during the dry season are also necessary.

In this study, we quantified the warming effect from GHG fluxes through the dry season from different mangrove zones. The selection of three prominent mangrove zones (*Rhizophora*, *Sonneratia*, *Bruguiera*) in the Ngurah Rai Grand Forest Park, Bali, was made to assess the overall state of the mangrove ecosystem accurately. This research aims to add data related to the seasonal fluctuations in GHG levels and their warming effect that have not been previously recorded in the same area. The research findings indicate that mangrove ecosystems also emit greenhouse gases (GHGs) from soil which increase the warming effect in the atmosphere, albeit in negligible amounts in this area. Because this is not the case in all mangrove areas GHG emissions need tobe known in order to calculate the blue carbon stock accurately. The research result also contributes to the FoLU (Forestry and Other Land Use) Net Sink 2030 program by collecting GHG data in the forestry sector in Indonesia.

2. METHODOLOGY

2.1 Study site and condition

This research is located in Ngurah Rai Forest Park, Bali (8°42'50.46"S, 8°47'49.92"S, 115°10'9.42"E, and 115°15'13.19"E). The majority of the mangrove forests have undergone conversion from shrimp ponds within the past three decades (JICA, 1999). Mangrove forests are primarily characterized by three primary genera: *Bruguiera*, *Rhizophora*, and *Sonneratia*. The general health of mangroves based on the mangrove health index (MHI) has been categorized as moderate (Sugiana et al., 2022). Fine sand dominates the mangrove soil in this area (Prinasti et al., 2020; Imamsyah et al., 2020). pH and salinity of the porewater vary across different zones depending on their proximity to the sea (Sugiana et al., 2021). A total of 12 study plots were allocated among the three mangrove zones, including 3 plots in the *Bruguiera* zone, 4 plots in the *Sonneratia* zone, and 5 plots in the *Rhizophora* zone (Figure 1). During the data collection, the weather conditions had clear skies, and the tide conditions reached their lowest point. The sampling time was carried out between August 23-28, 2023, in the daytime (1 pm to 3 pm; UTC+8 time zone). Data collection was only conducted once per plot. We also recorded the field air temperatures, which varied between 25.0 and 28.3°C (mean: 26.7°C), and humidity levels which ranged from 73 to 88% (mean: 80%).

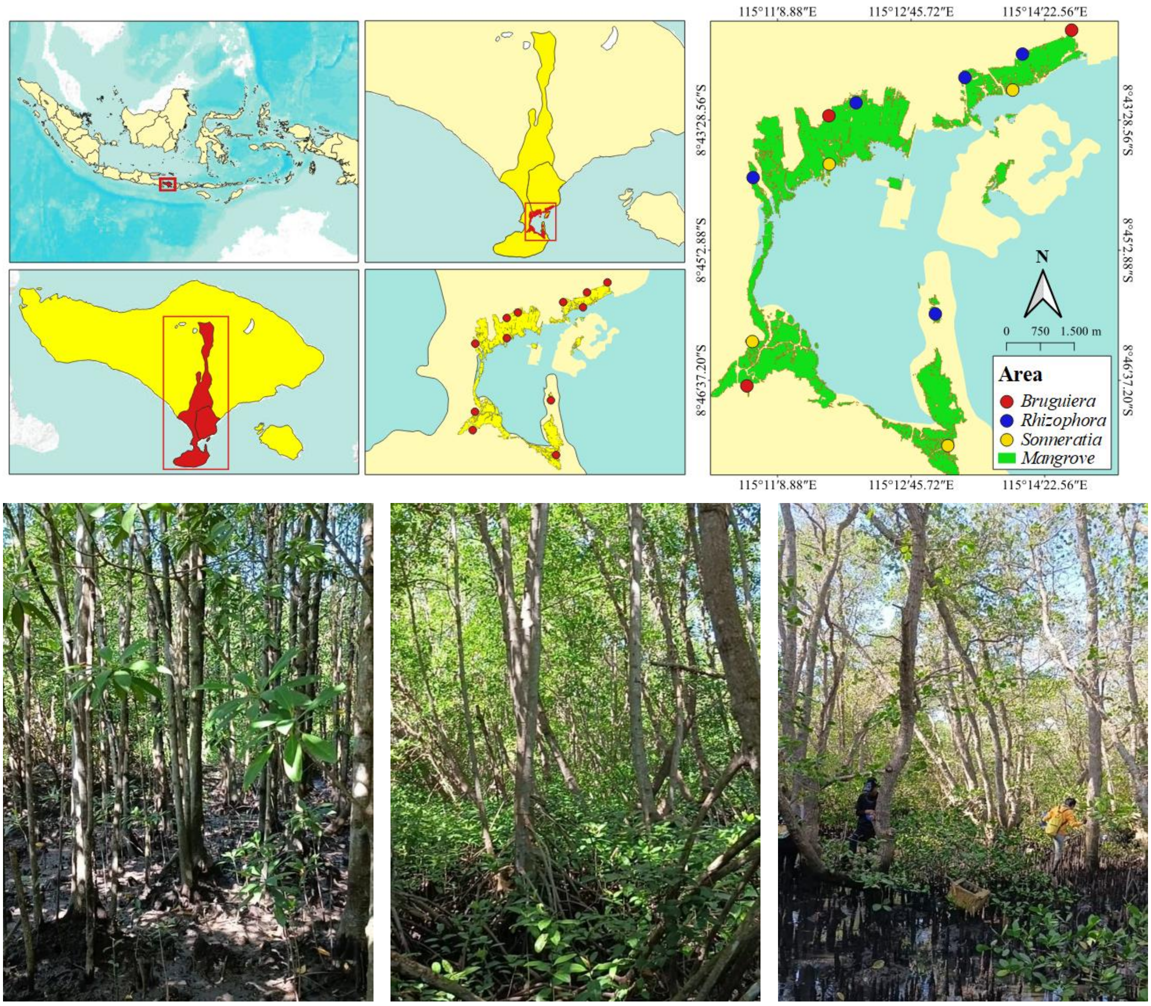

Bruguiera zone *Rhizophora* zone *Sonneratia* zone

Figure 1. Distributions and conditions of research data collection plots in Bali, Indonesia

The mangrove forest structure conditions and carbon sequestration rates vary across each mangrove zone, as shown in Table 1. The data for measuring the structure of the stand was collected following the guidelines for monitoring mangrove communities (Dharmawan and Ulumuddin, 2021). The carbon sequestration rates of each mangrove zone were derived by combining the parameters of stem diameter growth, burial rate, and litterfall production, yielding the annual rate of carbon sequestration. The data previously been published by Sugiana et al. (2024).

2.2 Greenhouse gases data collection

Each sampling plot has three subplots that serve as measuring points for GHG fluxes, positioned as shown in Figure 2. Each subplot is constrained by a 10×10 m transect that was previously employed to delimit measurements of the structure of mangrove stands. GHG samples were collected using a 10 mL syringe. The samples were taken after being incubated in a clear container constructed of acrylic, which had dimensions of 20×20×25 cm. The samples were collected at 10-minute intervals, four times in total (at t=0, 10, 20, and 30 minutes), following the methodology described by Chen et al. (2016). The incubation method involves submerging the chamber in mangrove soil, which is free from crab holes and debris, at a depth of around 2 cm. Gas samples were only collected in August 2023, marking the transitional period from the dry season to the rainy season. A total of 144 gas samples were collected from 12 plots, with each plot yielding twelve samples. The collected gas is transferred into a vacutainer tube with a capacity of 10 mL.

Table 1. Average forest structure of each mangrove zones and annual carbon sequestration rate

Parameter	Zone		
	Bruguiera	*Rhizophora*	*Sonneratia*
Dominance of mangrove	*B. gymnorrhiza*	*R. mucronata*	*S. alba*
Number of spp.	1	3	1
Tree density (stands/ha)	3,030	3,576	2,121
Sapling density (stands/ha)	1,414	1,333	985
Diameter at breast height (cm)	8.3	8.8	11.5
Canopy coverage (%)	75.18	74.59	49.17
Mangrove health index (%)	56.03	55.99	42.13
Carbon sequestration rate ($MgCO_2$/ha/year)	75.6	79.3	81.8

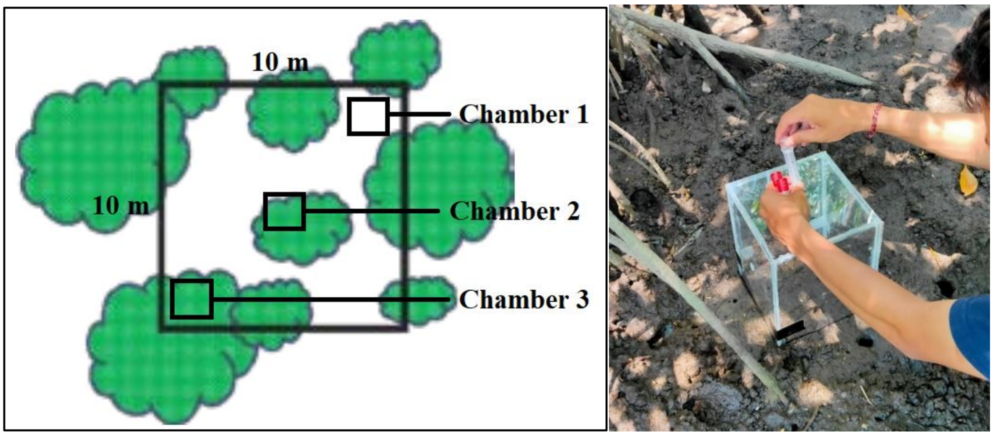

Figure 2. Position of incubation chamber between sampling plots (left; image is a modification from Dharmawan et al., 2020) and GHGs sampling (right)

The GHG samples were subsequently sent to the laboratory of the Agricultural Environmental Research Institute in Pati, Central Java, Indonesia to measure the concentration of each GHG. Determination of CH_4, CO_2, and N_2O in the samples was carried out using a gas chromatograph (450-GC Varian) was used. This machine had a flame ionization detector (FID), a thermal conductivity detector (TCD), and a ^{63}Ni electron capture detector (μECD). The 450-GC Variant is further furnished with a PAL autosampler injector that operates as an auto-injector with a capacity of 2 mL. It utilizes Ar, H_2, He, and N_2 as carrier gases. The measuring procedure was conducted at a temperature of 25°C, and the obtained measurements are compared to a standard curve that serves as a reference. The determination of concentration values is derived by comparing the peak area with the value obtained from the standard curve. Subsequently, the concentrations of CO_2, CH_4, and N_2O are transformed into flux values by applying the equation derived by Chen et al. (2016):

$$Fm = \frac{V \times \Delta M \times 10^6}{A \times P} \quad (1)$$

Where; Fm=GHG fluxes (μg/m^2/h), ΔM=the slope of the linear regression line between GHG concentrations (ppm) and sampling frequency (10 min transformed to an hour), V=chamber volume (L), A= chamber area (m^2), P=constant gas volume (22.414 L/mol).

The CH_4 and N_2O fluxes are transformed into CO_2-equivalent form in order to standardize their warming impact with that of CO_2 by using the following formula:

$$Fe = Fm \times M \times GMP \quad (2)$$

Where; Fe=warming effect in CO_2-equivalent fluxes (gCO_2/m^2/h converted to $MgCO_2$/ha/year), Fm=GHG fluxes (mol/m^2/h), M=molecular weight of the GHGs (CH_4: 16.04 g/mol and N_2O: 44.013 g/mol), GMP=warming effect or the conversion factor of CH_4 and N_2O emissions to CO_2 equivalents as 29.8 and 273, respectively, over a 100-year timeframe (IPCC, 2021).

2.3 Soil and porewater physicochemical characteristics measurement

Environmental condition measurement is divided into two components: soil and porewater. We collected the soil sample using a soil auger with a diameter of 5 cm at a depth ranging from 0 to 100 cm. Subsequently, the soil pH was measured using a Lutron 212 pH meter. We first homogenized the soil, and then 300 grams were collected and stored in plastic containers. One hundred grams of soil samples were dried at 70°C until a consistent weight was achieved (approximately 48 h) to obtain the percentage of the water content. We also dried another 100 g of the soil at 105°C to measure the bulk density value. A dried soil used for water content measurement is then used again for grain size analysis (10 g), soil organic carbon (SOC) measurement (3 g), and the rest (around 100 g) for total Kjeldahl nitrogen (TKN) and phosphorus (TP) analysis. We used the dry sieve method (gravel: 2 mm, sand: 1.1 mm-75 µm) and the settling time method for silt and clay categorization for soil grain size analysis. For SOC, we used the loss on ignition (LOI) method, where the samples were burned at a temperature of 550°C (Chen et al., 2014). TKN analysis was performed using a flow injection analyzer (FIA) method, and TP was measured using the colorimetric persulfate digestion method. Since the data collection was conducted during low tide, porewater samples were mostly found at 50-100 cm from the soil surface. We measured several parameters, including temperature, pH, salinity, and ORP, using the Multimeter COM-600 Water Quality Tester, and the dissolved oxygen (DO) was measured using a Lutron DO-5519 meter. The soil sampling for these measurements was performed after the GHG samples were collected to avoid soil disturbance affecting the GHG data.

2.4 Statistical analysis

We used ANOVA analysis to see if there are notable disparities in GHG emission rates and environmental variables, specifically soil and porewater. All the data, including GHG production rates, mangrove stand structure, carbon sequestration, and ecological condition, had a normal distribution ($\rho>0.05$) based on the Shapiro-Wilk test. We then used the Tukey Honestly Significant Difference (HSD) follow-up test to determine the zones that exhibited statistically significant differences. A Pearson correlation test was also performed using R Studio version 4.0.2 software to establish the relationship between GHG flux and mangrove ecological parameters (stand structure and environment condition). Principal component analysis (PCA) with MVSPW software was used to determine the correlation among all parameters and GHG emission in the study areas.

3. RESULTS AND DISCUSSION

3.1 Soil and porewater physicochemical characteristics

Generally, each mangrove zone is categorized by the predominant sandy soil type. According to Shepard’s categorization, the soil composition varies, ranging from primarily sandy (with a sand content of at least 75%) to a mixture of sand and silt/clay known as sandy loam (with a sand content between 50-75% and a combined silt and clay content of at least 25%) (Table 2). In detailed information, the main soil types are categorized into four: rough sand, medium sand, fine sand, and very fine sand. Fine sand dominated the *Bruguiera* and *Sonneratia* zones by 38.7% and 19.3%, respectively, while medium sand dominated the *Rhizophora* zone by 22.5% (Figure 3).

No soil properties, including pH, moisture content, bulk density, SOC, TKN, TP, C:N, and N:P Ratio, show significant differences based on the ANOVA test ($\rho>0.05$). However, when looking at the average values, the highest values for soil pH, water content, SOC, and C:N Ratio were found in the *Sonneratia* zone, while the lowest was in the *Rhizophora* zone (Table 2). Furthermore, the bulk density and total phosphorus are higher in the *Bruguiera* zone, while the TN and N:P ratios are highest in the *Rhizophora* zone (Table 2).

The discrepancies in values among soil properties can be attributed to their interdependent relationship. The *Sonneratia* zone, characterized by greater clay content, exhibits the highest organic carbon levels. This is because clay soil can bind carbon tightly more than coarser soil types (Matus, 2021; Amorim et al., 2023). Similarly, the lower bulk density value relates to a higher presence of organic carbon, indicating an inverse relationship with soil organic carbon concentration (Perie and Ouimet, 2008; Matus, 2021). Soil that contains a high amount of organic material has a greater capacity to absorb water, resulting in higher water content values (Gao et al., 2019). Given its proximity to these water sources, the *Sonneratia* zone exhibits a slightly higher soil pH, perhaps due to the influx of surface water from the nearby sea and neighboring rivers (Figure 4). Microbial metabolic activities, specifically nitrification and denitrification processes, and the dark cycle process of photosynthesis in plants, can cause minor fluctuations in TKN and TP content. These processes indirectly involve the utilization of nitrogen and phosphorus available in the soil (Lovelock et al., 2006; Inoue et al., 2011; Zhu et al., 2013; Queiroz et al., 2019).

Table 2. Comparison of GHG fluxes in mangroves soil of Ngurah Rai Forest Park, Bali with other regions (NA: not available)

Location	Dominated mangrove species	Region	GHG Fluxes (µg/m^2/h)			References
			CO_2	CH_4	N_2O	
Ngurah Rai Forest Park, Bali (Dry season)	*Bruguiera, Rhizophora, Sonneratia*	Tropical	322.5-3,494.5	-24.7-60.9	-1.2-2.32	This study
Ngurah Rai Forest Park, Bali named as Benoa Bay, Bali (Wet season)	*Bruguiera, Rhizophora, Sonneratia*	Tropical	98-8,953	0.9-88.0	0.24-3.6	Sugiana et al. (2023)
Tampamachoco coastal lagoon, Mexico	*Avicennia germinans*	Tropical	-242.9-358	-3.0-5.6	-1.1-2.9	Romero-Uribe et al. (2022)
Budai, Taiwan	*Kandelia, Avicennia*	Sub-Tropical	NA	14.1-316.9	NA	Lin et al. (2020)
Honda bay, Philipines	*Rhizophora*	Tropical	252-33,300	-5.95-17.53	-0.67-5.54	Castillo et al. (2017)
Bhitarkanika, India	*Rhizophora*	Sub-Tropical	NA	5	0.20	Chauhan et al. (2015)
Sulawesi, Indonesia	*Rhizophora, Bruguiera*	Tropical	-1,340-3,880	-6.1-13.1	-0.35-0.61	Chen et al. (2014)
Maipo, Hongkong	*Kandelia, Acanthus*	Sub-Tropical	31	NA	11.6	Chen et al. (2012)
Futian, China	*Kandelia, Acanthus, Bruguiera*	Sub-Tropical	-560-20.6	10.1-5,168.6	0.14-23.8	Chen et al. (2010)
Brisbane, Australia	*Avicennia, Aegiceras*	Sub-Tropical	NA	272.5	40.4	Allen et al. (2007)

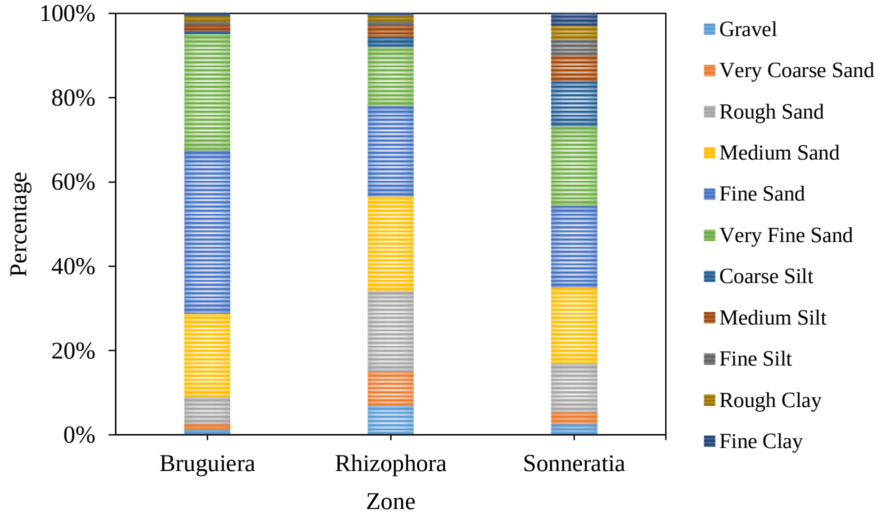

Figure 3. Soil type classification from each mangrove zone in TAHURA Ngurah Rai, Bali

Several porewater parameters, including salinity, oxidation-reduction potential (ORP), and dissolved oxygen (DO), demonstrate substantial differences (ρ<0.05) across mangrove zones. However, the rest of the parameters were not significantly different (ρ>0.05). The *Bruguiera* zone had the highest average temperature, salinity, ORP, and DO values in porewater, whereas the *Sonneratia* zone displayed the lowest values. Unlike other conditions, pH levels are high in the Sonneratia zone and low in the *Rhizophora* zone. This pattern is also observed in soil pH, as shown in Table 3.

Figure 4. Fresh water irrigation flows were found at the two southernmost *Sonneratia* plots

Table 3. Soil and porewater properties of each mangrove zone

Media	Parameter	Zone		
		Bruguiera	*Rhizophora*	*Sonneratia*
Soil	Dominant soil type	Sand (Gravel: 1%, Sand: 94%, Silt: 3%, Clay: 2%)	Sand (Gravel: 7%, Sand: 85%, Silt: 6%, Clay: 2%)	Sandy Loam (Gravel: 3%, Sand: 71%, Silt: 21%, Clay: 6%)
	Soil pH	6.32±0.25[a]	6.23±0.22[a]	6.66±0.26[a]
	Water content (%)	42.8±2.9[a]	37.4±4.8[a]	50.9±12.5[a]
	Bulk density (g/cm^3)	0.81±0.16[a]	0.80±0.06[a]	0.66±0.07[a]
	Soil organic carbon (SOC) (%)	1.24±0.47[a]	1.16±0.40[a]	1.96±0.36[a]
	Total Kjeldahl Nitrogen (TKN) (%)	0.05±0.04[a]	0.06±0.02[a]	0.05±0.03[a]
	Total phosphor (TP) (%)	0.013±0.001[a]	0.009±0.003[a]	0.012±0.002[a]
	C:N ratio	47.9±35.5[a]	21.3±6.4[a]	50.0±24.0[a]
	N:P ratio	3.8±3.8[a]	7.0±3.2[a]	4.2±2.8[a]
Porewater	Temperature (°C)	28.3±1.0[a]	27.8±0.9[a]	27.5±0.6[a]
	pH	6.43±0.17[a]	6.37±0.19[a]	6.81±0.34[a]
	Salinity (ppt)	22.94±1.94[a]	22.19±1.00[ab]	19.50±2.07[b]
	ORP (mV)	6±53[a]	-58±29[ab]	-95±59[b]
	Dissolved oxygen (DO) (mg/L)	2.44±0.71[a]	1.30±0.38[b]	1.25±0.36[b]

Similar to soil conditions, porewater properties are also related each other. High porewater pH in the *Sonneratia* zone may be caused by the flushing of tides or the proximity of river flow near the monitoring area (Figure 4). This also caused low salinity values found in the same zone. Generally, *Bruguiera* mangroves grow near land with low salinity conditions (Dangremond et al., 2015). However, this condition was found due to multiple measurement locations inside the area predominantly occupied by the *Sonneratia* species with low porewater salinity. This caused the *Bruguiera* zone to have the highest salinity value compared to the *Sonneratia* zone. The *Sonneratia* zone also has lower levels of ORP and DO, which can be attributed to the breakdown of organic matter by high aerobic microbial metabolism. Consequently, the soil in mangrove areas tends to have a reducing tendency, as seen by negative ORP values (Hall et al., 2013).

3.2 Soil greenhouse gas fluxes

No significant variations were found between mangrove zones in the CO_2, CH_4, and N_2O fluxes ($\rho>0.05$). The average CO_2 flux in the *Bruguiera* and *Sonneratia* zones is twice as high as in the *Rhizophora* zone, measuring 2,660.0±611.9 µg/m^2/h and 2,456.1±1,261.1 µg/m^2/h, respectively. The *Sonneratia* zone produced 35.4±17.4 µg/m^2/h CH_4 gas, while the *Bruguiera* and *Rhizophora* zones only comprised 7% and 21% of the average CH_4 gas production compared to the *Sonneratia* zone. However, while considering the N_2O flux, it was seen that the *Rhizophora* zone had the highest flux value, specifically 0.6±0.9 μg/m^2/h. This value was 1.2 times higher than in the *Bruguiera* zone and six times higher than in the *Sonneratia* zone (Figure 5).

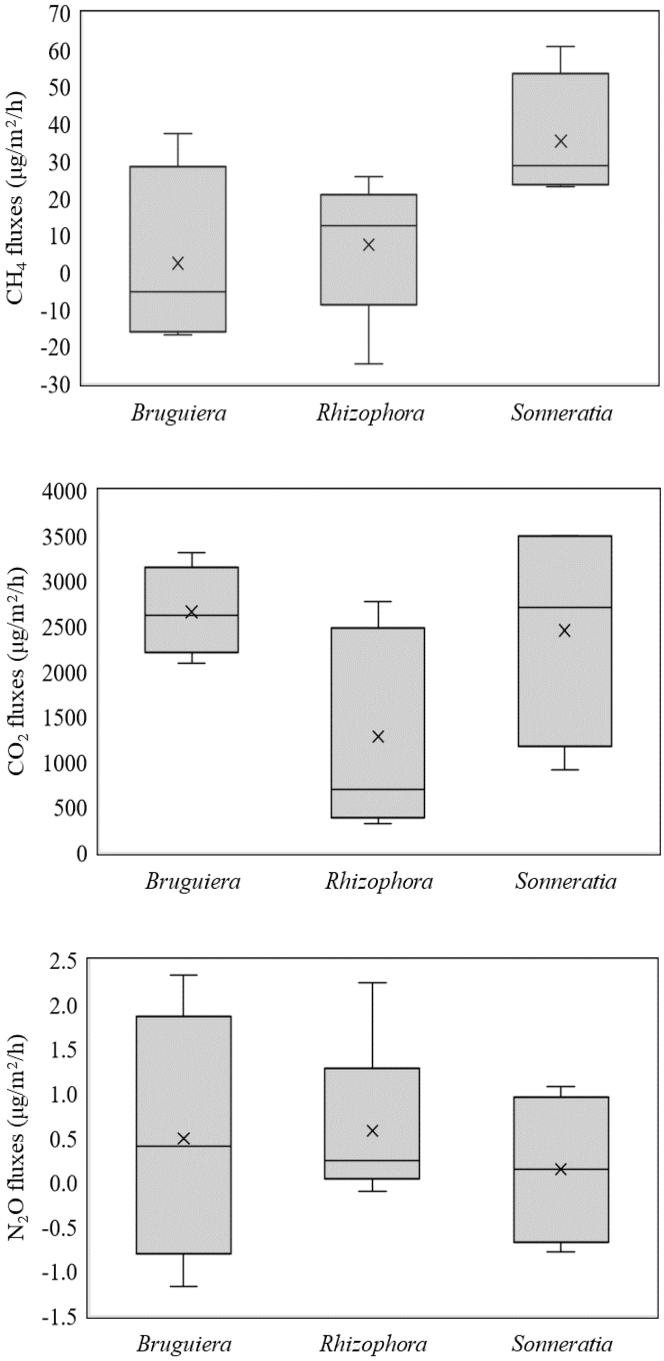

Figure 5. Greenhouse gas fluxes of each mangrove zone in TAHURA Ngurah Rai, Bali

Other study have shown that mangrove soil can act as both sources (positive value) and sinks (negative value) of GHGs (Konnerup et al., 2014; Atwood et al., 2017; Cabezas et al., 2018; Romero-Uribe et al., 2022). There is no discernible pattern in the GHG fluxes trend between mangrove zones. Nevertheless, a positive trend of CO_2 fluxes demonstrates that mangrove soil always emits CO_2 into the atmosphere. Meanwhile, the CH_4 and N_2O fluxes exhibit inconsistent trends, varying between positive and negative values. Most GHG fluxes with negative values were seen in the *Bruguiera* zone for CH_4 and the *Sonneratia* zone for N_2O. The maximum and minimum CH_4 flux values throughout all mangrove zones are 60.85 μg/m^2/h and -24.67 μg/m^2/h, while N_2O fluxes are 2.25 μg/m^2/h and -1.17 μg/m^2/h, respectively. CH_4 and N_2O fluxes can exhibit negative values in certain instances, as observed in studies conducted in North Sulawesi, Indonesia (Chen et al., 2014) and Tampamachoco coastal lagoon, Mexico (Romero-Uribe et al., 2022). This phenomenon is mostly attributed to microbial activity and environmental conditions.

Wetland soil, including mangrove ecosystems, mostly has high organic matter with limited oxygen. Methanogenic bacteria produce more CH_4 gas in anaerobic conditions. Conversely, when there is an ample oxygen supply, CO_2 is predominantly produced (Adame and Lovelock, 2011; Chen et al., 2016; Sugiana et al., 2023). The CH_4 flux may vary due to environmental conditions or the presence of specific microbes in the soil, particularly methanogenic (methane producer) and methanotrophic (methane consumer) bacteria. Methanotrophic bacteria utilize CH_4 as an energy source and metabolize it into methanol and then formaldehyde which is subsequently metabolized further to produce carbon-containing biomass and CO_2 (Kalyuzhnaya et al., 2019; Nazir and Zaffar, 2021). When the activity of methanotrophic bacteria exceeds that of methanogenic bacteria, the CH_4 production will drop. For example, in the *Bruguiera* zone, where oxygen levels are high, methane production is generally lower than in other zones.

In addition, N_2O is a greenhouse gas produced by bacteria during the denitrification process in anaerobic environments (Marton et al., 2012; Queiroz et al., 2019). The energy requirements for microbial adaptation and the stability of nitrogen molecules influence the production of N_2O. The primary conversion of N_2O to N_2 instead of the formation of N_2O from nitrogen monoxide (NO) leads to a decline in N_2O production in the soil. As a result, measurements of N_2O flux sometimes provide negative values or demonstrate a downward trend. Denitrifying bacteria rely on nitrous oxide (N_2O) molecules as electron acceptors during anaerobic respiration to generate energy. The breakdown of N_2O into N_2 liberates a greater amount of energy, hence facilitating the proliferation and viability of bacteria (Conrad, 1996; Zumft and Kroneck, 2006; Ussiri and Lal, 2013). In addition, N_2 is more stable than other nitrogen forms, leading to higher production quantities in this form (Robertson and Groffman, 2024).

Multiple research studies have demonstrated varying levels of GHG fluxes. Despite their shared tropical locations, GHG emissions exhibit significant variability. This is also true in other sub-tropical regions, as indicated in Table 2. We found that GHG fluxes in Ngurah Rai Forest Park, Bali, are lower during the dry season compared to the wet season. These findings demonstrate that fluctuations in GHG emissions are also influenced by seasonal factors, similar to other studies conducted in the Ayeyarwady Delta, Myanmar (Cameron et al., 2021) and Sudarban, India (Padhy et al., 2020). In addition, the features of the mangrove type also appear to impact the rate of greenhouse gas flux indirectly. Table 2 demonstrates that various research locations are primarily characterized by a specific type of mangrove, resulting in distinct GHG emissions compared to other areas dominated by different mangrove species. However, despite being predominantly influenced by the Rhizophoraceae group in Sulawesi, Indonesia, and Honda Bay, Philippines, the greenhouse gas (GHG) emissions show notable disparities compared to the current findings. This suggests that more factors, such as hydro-oceanic conditions, affect GHG fluxes.

3.3 Soil GHG relationship with environmental parameters

We found no relationship between atmospheric conditions and GHG fluxes. However, stand structure, sapling density seems to correlate with N_2O flux. Most soil properties, including water content, bulk density, TOC, TKN, C:N ratio, N:P ratio, and soil types, have positive or negative correlations with GHG fluxes. The pore water characteristics did not significantly correlate with GHG fluxes, as indicated in Table 4.

The correlation between the sapling density and the N_2O flux can be attributed to the state of the roots of mangrove plants. Increased sapling density leads to a greater accumulation of organic matter, including nitrogen, in the soil, which bacteria can exploit to create N_2O gas (Xiong et al., 2017; Alongi, 2020). In addition, high sapling density leads to greater soil stability and enhanced microbial diversity, all of which contribute to the production of N_2O (Braker and Conrad, 2011; Craig et al., 2021).

Low bulk density with high sand composition (mostly mineral content) can indicate high CO_2 production (Chen et al., 2016; Yost and Hartemink, 2019; Sugiana et al., 2023). Sandy soil has a looser porosity, making it easier for dissolved oxygen to enter the porewater. Meanwhile, a low bulk density with silty and clayed soil, mostly with high water content, indicated a high TOC concentration used to produce CO_2 gas through microbial activity (Matus, 2021; Amorim et al., 2023). However, it also triggers high CH_4 production because silt and clay soil reduce dissolved oxygen levels in porewater, causing anoxic environmental conditions (Wang et al., 2009; Gao et al., 2019; Liu et al., 2020; Matus, 2021).

Table 4. Pearson correlation coefficient values (r) among atmospheric condition, mangrove structure, soil, and porewater properties with greenhouse gases (*=correlation coefficient at ρ<0.05, while ** at ρ<0.01)

Parameter	Correlation coefficient		
	CO_2	CH_4	N_2O
Atmospheric condition			
Temperature (°C)	0.13	0.28	-0.04
Humidity (%)	-0.41	-0.37	-0.05
Mangrove structure			
Tree density (ind/ha)	-0.27	-0.31	-0.08
Sapling density (ind/ha)	-0.36	-0.18	**0.59***
Diameter (cm)	0.57	0.33	-0.16
Canopy cover (%)	-0.44	0.05	0.21
Health index (%)	-0.46	-0.03	0.19
Soil properties			
Soil pH	0.09	0.02	0.32
Water content (%)	0.57	**0.59***	-0.02
Bulk density (g/cm^3)	**-0.74****	**-0.58***	0.46
TOC (%)	**0.72****	**0.74****	-0.31
TKN (%)	-0.06	0.09	**0.87****
TP (%)	0.18	0.12	-0.24
C:N Ratio	0.27	0.30	**-0.73****
N:P Ratio	-0.09	0.05	**0.69***
Gravel (%)	-0.36	**-0.93****	0.11
Sand (%)	**-0.65***	**-0.59***	0.04
Silt (%)	**0.64***	0.51	-0.06
Clay (%)	**0.75****	**0.69***	-0.17
Porewater properties			
Temperature (°C)	-0.43	0.03	0.42
pH	0.36	0.03	0.10
Salinity (ppt)	-0.35	-0.02	0.02
ORP (mV)	-0.17	0.11	0.23
DO (mg/L)	-0.25	0.27	0.44

Only three soil properties, including TKN, C:N ratio and N:P ratio, strongly correlate with N_2O flux. Nitrogen availability in mangrove soil is an energy source for denitrifying bacteria to produce N_2O gas (Queiroz et al., 2019). Measured TKN includes organic nitrogen and also ammonium (NH_4^+) and ammonia (NH_3). Since N_2O flux highly correlates with TKN, it shows that nitrification and denitrification processes in the nitrogen cycle are occurring in the mangrove ecosystem. The nitrification process converts NH_4^+ and NH_3 into nitrate (NO_3), while denitrification converts NO_3 into nitrite (NO_2^-)- > NO- > N_2O- > N_2 (stable) (Robertson and Groffman, 2024).

In addition, another parameter could have a significant relationship with GHG fluxes in different conditions and locations. Vegetation stand structure and composition may impact GHG fluxes indirectly since they could affect soil organic matter production. A high density of mangrove stands and canopy cover leads to higher organic matter, including TOC and TN, which are the sources of GHG production (Weiss et al., 2016; Alongi, 2020; Dermawan et al., 2023). Soil and porewater pH are also one of the important indicators, especially for CH_4 production. A low pH value could show high CH_4 production due to anoxic conditions (Koebsch et al., 2013; Ulumuddin, 2018). Porewater ORP and DO are also other crucial parameters. CO_2 is mostly produced when their values increase, while low ORP and DO will cause increased fluxes of CH_4 and N_2O. Temperature also plays a crucial role in influencing the rate of micrometabolic processes, thereby impacting variations in GHG production. Another last parameter that could affect GHG production is salinity. Salinity often affects CH_4 synthesis by enhancing the activity of sulfate-reducing bacteria, which compete with methanogens for resources (Chen et al., 2014; Welti et al., 2017; Sugiana et al., 2023).

The first principal component (PC1) explains 55.161% of the total variance, while the second principal component (PC2) accounts for 22.579% of the variance. Together, these components explain 77.74% of the total variability, which indicates that the two principal components effectively capture the primary patterns in the data. Sapling Density shows a strong positive contribution to both PC1 and PC2, suggesting that areas with higher sapling density are significantly distinct in terms of the environmental variables considered. N_2O contributes positively to PC2, implying that higher N_2O levels are associated with variations captured by the second principal component. CO_2, Clay, TOC, and CH_4 exhibit strong positive contributions to PC1, indicating that these variables are closely related and influence the first principal component. C:N has a strong negative contribution to PC1, suggesting that lower C:N are characteristic of the environmental gradient represented by PC1.

Bruguiera plots (represented by red triangles) predominantly cluster in the negative quadrant of PC1, except for B1 (Figure 6). This clustering suggests that *Bruguiera* dominated area are associated with environments characterized by lower levels of CO_2, Clay, TOC, and CH_4, but higher C:N. *Rhizophora* plots (depicted by blue triangles) are distributed across the negative sides of both PC1 and PC2, with the exception of R5, indicating that these species are adapted to environments with lower levels of most considered environmental variables. *Sonneratia* plots (represented by yellow squares) exhibit a broader distribution across the biplot. S4 and S2 plots are positioned in the positive quadrant of PC1, suggesting that *Sonneratia* dominated area are more tolerant of or associated with higher levels of CO_2, Clay, TOC, and CH_4. These results indicate that mangrove soil dominated by *Sonneratia* may exhibit both oxic and anoxic conditions, as indicated by high production of CO_2 and CH_4.

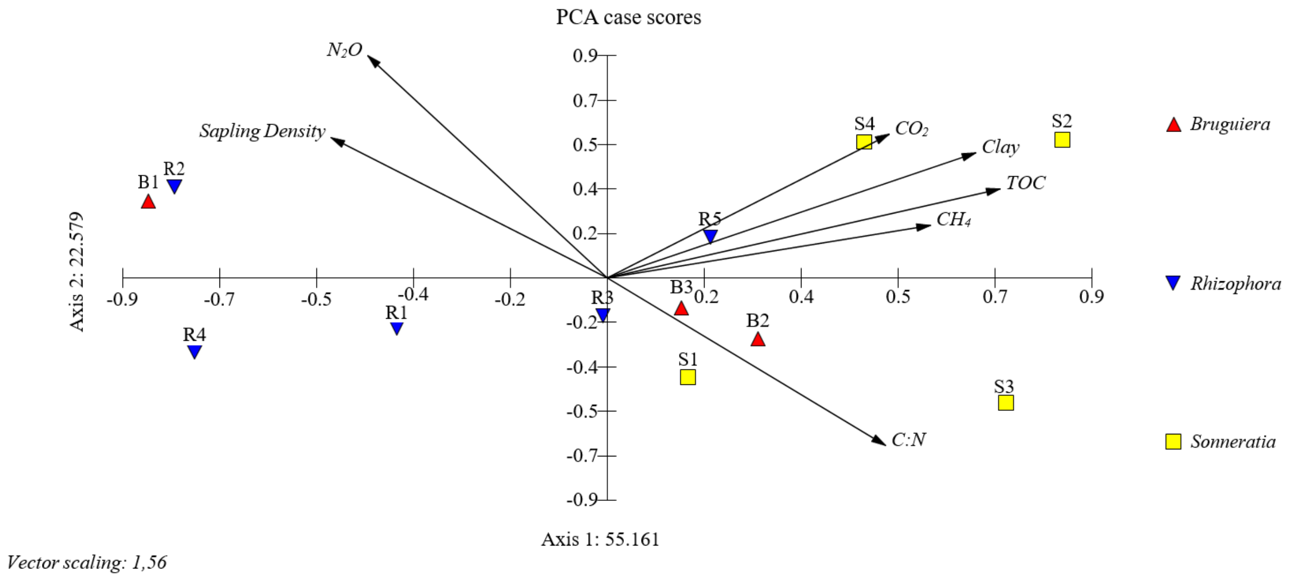

Figure 6. PCA analysis result of GHG fluxes and mangrove ecological parameters (B: *Bruguiera*, R: *Rhizophora* and S: *Sonneratia* zones)

3.4 Contribution to warming effect

The average GHG flux value of CO_2-equivalent (warming effect) showed positive results across mangrove zones but with a high variability. N_2O is the primary factor contributing to high warming in the *Bruguiera* and *Rhizophora* zones, while CH_4 is the major contributer in the *Sonneratia* zone. The *Sonneratia* zone has emerged as the primary driver of the warming effect, contributing the highest amount of 1.8±1.4 $MgCO_2$/ha/year (Table 5).

Compared to other studies, the global warming effect of GHG fluxes from mangrove sediments in Bali's Ngurah Rai Forest Park is relatively low. In Sulawesi, Indonesia, with an almost similar mangrove zonation, the warming effect from mangrove soil GHGs is nearly 16 times greater than this result (Table 6). This demonstrates that factors other than the mangrove genera zonation pattern affect GHG emissions. We have summarised several comparisons of the warming effect of each GHG in several regions of the world, as shown in Table 6.

Table 5. Soil greenhouse gases warming effect from each mangrove zones in Ngurah Rai Forest Park, Bali, Indonesia

Zone	CO_2-equivalent flux ($MgCO_2$/ha/year)			
	CO_2	CH_4	N_2O	Total
Bruguiera	0.2±1.3	0.1±0.1	0.5±1.9	0.9±1.1
Rhizophora	0.1±0.8	0.3±0.1	0.6±1.0	1.0±1.3
Sonneratia	0.2±0.7	1.5±0.1	0.2±0.9	1.8±1.4
Average	0.2±1.0	0.6±0.1	0.4±1.1	1.2±1.2

Table 6. Warming effect of soil greehouse gases from several regions (NA: data not available)

Region	Condition	Warming effect ($MgCO_2$/ha/year)			Total	References
		CO_2	CH_4	N_2O		
Ngurah Rai Forest Park, Bali, Indonesia	Peak of dry season (August), three dominated genera	0.6±0.1	0.2±1.0	0.4±1.1	1.2±1.2	This study
	Wet season (December) three dominated genera	0.2±0.1	0.6±0.4	1.1±0.4	1.9±0.7	Sugiana et al. (2023)
Ayeyarwady Delta, Myanmar	Dry season (February)	8±0.5	0.2±0.1	1.6±0.3	9.8±0.9	Cameron et al. (2021)
	Wet season (October)	78.5±16.2	0.3±0.1	NA	78.8±16.3	
North Sulawesi, Indonesia	High *Ceriops tagal*/*R. apiculata*/*S. alba* covers, 10 years old mangroves	25.7±2	3.1±0.5	0.7±0.3	29.5±2.8	Cameron et al. (2019)
South Sulawesi, Indonesia	*R. apiculata*/*S. alba*/*B. gymnorrhiza* dominated zone	16.7±0.8	1.4±0.2	1.3±0.1	19.4±1.1	Cameron et al. (2019)
	Inudated, operating ponds	0.5±0.0	0.6±0.3	NA	1.1±0.2	
Perancak Estuary, Bali, Indonesia	*Avicennia*, *Rhizophora*, *Sonneratia*, and *Bruguiera* dominated zones	44.8±6.6	NA	NA	44.8±6.6	Sidik et al. (2019)
Northern Vietnam	*Kandelia candel* dominated site	15.3±14.3	NA	NA	15.3±14.3	Hien et al. (2018)
Honday Bay, Philippines	Abandoned pond with little regrowth mangroves	15.9±3.7	NA	NA	15.9±3.7	Castillo et al. (2017)
Global average of mangrove forest	Sum of autotrophic and heterotrophic respiration	17.6	19.5	NA	19.5	Alongi (2014)

Compared to the rate of CO_2 sequestration (as shown in Table 1), which effectively decreases the warming impact on the atmosphere, the proportion of greenhouse gas emissions to CO_2 storage rate is only approximately 1.1-2.2% for all the mangrove zones in Ngurah Rai Forest Park. Therefore, the emission of GHG does not substantially impact the mangrove ecosystem's ability to mitigate global warming. Consequently, it can be disregarded when calculating the carbon stock in the case of the mangrove ecosystem in Ngurah Rai Forest Park, Bali. However, to determine the significance of the warming impact value, conducting a thorough and evaluation is imperative. Multiple studies have shown that the warming effect value can account for up to 20.5% of the overall carbon sequestration rate in the mangrove ecosystem in China, specifically in areas dominated by the genus Kandelia (Chen et al., 2016). Furthermore, considering only CH_4 emissions, the warming effect value can reach as high as 24% (Liu et al., 2020). Zoning characteristics and the environmental conditions that facilitate greenhouse gasses (GHGs) production can contribute to this variation (Zhu et al., 2013).

4. CONCLUSION

In summary, there are no substantial variations in soil GHG fluxes across mangrove zones. Mangrove soil can function as both sources and sinks of GHGs. The flux of GHGs is closely associated with several parameters, such as SOC, TKN, water content, bulk density, and soil type. CH_4 significantly contributed to the *Sonneratia* zone's warming effect, while N_2O was the major contributor in the other two zones. Soil GHGs warming effect only reduces small amounts of mangrove ecosystem effectivness in mitigating global warming. Hence, the impact of greenhouse gas emissions in each mangrove zone can be disregarded when estimating the carbon stock at TAHURA Ngurah Rai, Bali.

ACKNOWLEDGEMENTS

We express our gratitude to the Indonesian Ministry of Education, Culture, Research, and Technology (Kemendikbudristek) for providing financial support for this research project under the master's thesis research plan (18930/IT3.D10/PT.01.02/M/T/2023). We also thank Putri, Nova, Echa, Ilham, and Wahyu for their valuable contributions in collecting field data and Dr. Bruce Campbell for his help in improving the English grammar in this paper. The authors declare no conflict of interest in preparing this paper.

REFERENCES

Adame MF, Lovelock CE. Carbon and nutrient exchange of mangrove forests with the coastal ocean. Hydrobiologia 2011;663:23-50.

Allen DE, Dalal RC, Rennenberg H, Meyer RL, Reeves S, Schmidt S. Spatial and temporal variation of nitrous oxide and methane flux between subtropical mangrove sediments and the atmosphere. Soil Biology and Biochemistry 2007;39(2):622-31.

Alongi DM. Carbon cycling and storage in mangrove forests. Annual Review of Marine Science 2014;6:195-219.

Alongi DM. Nitrogen cycling and mass balance in the world's mangrove forests. Nitrogen 2020;1(2):167-89.

Amorim HC, Araujo MA, Lal R, Zinn YL. What C:N ratios in soil particle-size fractions really say: N is preferentially sorbed by clays over organic C. Catena 2023;230:Article No. 107230.

Atwood TB, Connolly RM, Almahasheer H, Carnell PE, Duarte CM, Ewers Lewis CJ, et al. Global patterns in mangrove soil carbon stocks and losses. Nature Climate Change 2017; 7(7):523-8.

Braker G, Conrad R. Diversity, structure, and size of N_2O-producing microbial communities in soils: What matters for their functioning? Advances in Applied Microbiology 2011; 75:33-70.

Bunting P, Rosenqvist A, Lucas RM, Rebelo LM, Hilarides L, Thomas N, et al. The global mangrove watch: A new 2010 global baseline of mangrove extent. Remote Sensing 2018; 10(10):Article No. 1669.

Cabezas A, Mitsch WJ, MacDonnell C, Zhang L, Bydałek F, Lasso A. Methane emissions from mangrove soils in hydrologically disturbed and reference mangrove tidal creeks in southwest Florida. Ecological Engineering 2018;114:57-65.

Cameron C, Hutley LB, Friess DA. Estimating the full greenhouse gas emissions offset potential and profile between rehabilitating and established mangroves. Science of the Total Environment 2019;665:419-31.

Cameron C, Hutley LB, Munksgaard NC, Phan S, Aung T, Thinn T, et al. Impact of an extreme monsoon on CO_2 and CH_4 fluxes from mangrove soils of the Ayeyarwady Delta, Myanmar. Science of the Total Environment 2021;760:Article No. 143422.

Castillo JAA, Apan AA, Maraseni TN, Salmo SG. Soil greenhouse gas fluxes in tropical mangrove forests and in land uses on deforested mangrove lands. Catena 2017;159:60-9.

Chauhan R, Datta A, Ramanathan AL, Adhya TK. Factors influencing spatio-temporal variation of methane and nitrous oxide emission from a tropical mangrove of eastern coast of India. Atmospheric Environment 2015;107:95-106.

Chen G, Chen B, Yu D, Tam NF, Ye Y, Chen S. Soil greenhouse gas emissions reduce the contribution of mangrove plants to the atmospheric cooling effect. Environmental Research Letters 2016;11(12):Article No. 124019.

Chen GC, Tam NF, Ye Y. Spatial and seasonal variations of atmospheric N_2O and CO_2 fluxes from a subtropical mangrove swamp and their relationships with soil characteristics. Soil Biology and Biochemistry 2012;48:175-81.

Chen GC, Tam NF, Ye Y. Summer fluxes of atmospheric greenhouse gases N_2O, CH_4 and CO_2 from mangrove soil in South China. Science of the Total Environment 2010; 408(13):2761-7.

Chen GC, Ulumuddin YI, Pramudji S, Chen SY, Chen B, Ye Y, et al. Rich soil carbon and nitrogen but low atmospheric greenhouse gas fluxes from North Sulawesi mangrove swamps in Indonesia. Science of the Total Environment 2014;487:91-6.

Conrad R. Soil microorganisms as controllers of atmospheric trace gases (H_2, CO, CH_4, OCS, N_2O, and NO). Microbiological Reviews 1996;60(4):609-40.

Craig H, Antwis RE, Cordero I, Ashworth D, Robinson CH, Osborne TZ, et al. Nitrogen addition alters composition, diversity, and functioning of microbial communities in mangrove soils: An incubation experiment. Soil Biology and Biochemistry 2021;153:Article No. 108076.

Dangremond EM, Feller IC, Sousa WP. Environmental tolerances of rare and common mangroves along light and salinity gradients. Oecologia 2015;179:1187-98.

Das N, Mondal A, Mandal S. Polluted waters of the reclaimed islands of Indian Sundarban promote more greenhouse gas emissions from mangrove ecosystem. Stochastic Environmental Research and Risk Assessment 2022;36: 1277-88.

Dermawan EP, Siregar YI, Efriyeldi E. Estimation of carbon reserves in sediments in the mangrove ecosystem of Bukit Batu Village, Bengkalis Regency, Riau. Asian Journal of Aquatic Sciences 2023;6(1):93-101.

Dewi IG, Faiqoh E, As-syakur AR, Dharmawan IW. Natural regeneration of mangrove seedlings in Benoa Bay, Bali. Journal of Tropical Marine Science and Technology 2021;13(3):395-410.

Dharmawan IWE, Ulumuddin YI, Prayudha B. Guide to Monitoring Mangrove Community Structure in Indonesia. Bogor, Indonesia: PT Media Sains Nasional; 2020.

Dharmawan IWE, Ulumuddin YI. Mangrove Community Structure Data Analysis, A Guidebook for Mangrove Health Index (MHI) Training. Makassar, Indonesia: NAS Media Pustaka; 2021.

Ewel K, Bourgeois J, Cole T, Zheng S. Variation in environmental characteristics and vegetation in high-rainfall mangrove forests, Kosrae, Micronesia. Global Ecology and Biogeography Letters 1998;7(1):49-56.

Gao Y, Zhou J, Wang L, Guo J, Feng J, Wu H, et al. Distribution patterns and controlling factors for the soil organic carbon in four mangrove forests of China. Global Ecology and Conservation 2019;17:e00575.

Hall SJ, McDowell WH, Silver WL. When wet gets wetter: Decoupling of moisture, redox biogeochemistry, and greenhouse gas fluxes in a humid tropical forest soil. Ecosystems 2013;16:576-89.

Hien HT, Marchand C, Aime J, Cuc NT. Seasonal variability of CO_2 emissions from sediments in planted mangroves (Northern Viet Nam). Estuarine, Coastal and Shelf Science 2018;213:28-39.

Imamsyah A, Bengen DG, Ismet MS. Structure and distribution of mangrove vegetation based on biophysical environmental quality in the Ngurah Rai Grand Forest Park, Bali. Ecotrophic 2020;14(1):88-99.

Inoue T, Nohara S, Matsumoto K, Anzai Y. What happens to soil chemical properties after mangrove plants colonize? Plant and Soil 2011;346:259-73.

Intergovernmental Panel on Climate Change (IPCC). Climate Change 2021: The Physical Science Basis. Contribution of Working Group I to the Sixth Assessment Report of the Intergovernmental Panel on Climate Change. Cambridge, USA: Cambridge University Press; 2021.

Japan International Cooperation Agency (JICA). The Final Report of Project Administration: The Development of Sustainable Mangrove Management Project Bali and Lombok, Republic of Indonesia. Jakarta, Indonesia: Ministry of Forestry and Estate Crops in Indonesia - Japan International Cooperation Agency; 1999.

Kalyuzhnaya MG, Gomez OA, Murrell JC. The methane-oxidizing bacteria (methanotrophs). In: McGenity T, editor. Taxonomy, Genomics and Ecophysiology of Hydrocarbon-Degrading Microbes: Handbook of Hydrocarbon and Lipid Microbiology. Switzerland: Springer Nature; 2019. p. 245-78.

Kitpakornsanti K, Pengthamkeerati P, Limsakul A, Worachananant P, Diloksumpun S. Greenhouse gas emissions from soil and water surface in different mangrove establishments and management in Ranong Biosphere Reserve, Thailand. Regional Studies in Marine Science 2022;56:Article No. 102690.

Koebsch F, Glatzel S, Jurasinski G. Vegetation controls methane emissions in a coastal brackish fen. Wetlands Ecology and Management 2013;21:323-37.

Konnerup D, Betancourt-Portela JM, Villamil C, Parra JP. Nitrous oxide and methane emissions from the restored mangrove ecosystem of the Ciénaga Grande de Santa Marta, Colombia. Estuarine, Coastal and Shelf Science 2014;140:43-51.

Kweku DW, Bismark O, Maxwell A, Desmond KA, Danso KB, Oti-Mensah EA, et al. Greenhouse effect: Greenhouse gases and their impact on global warming. Journal of Scientific Research and Reports 2018;17(6):1-9.

Lin CW, Kao YC, Chou MC, Wu HH, Ho CW, Lin HJ. Methane emissions from subtropical and tropical mangrove ecosystems in Taiwan. Forests 2020;11(4):Article No. 470.

Liu J, Zhou Y, Valach A, Shortt R, Kasak K, Rey-Sanchez C, et al. Methane emissions reduce the radiative cooling effect of a subtropical estuarine mangrove wetland by half. Global Change Biology 2020;26(9):4998-5016.

Lovelock CE, Feller IC, Ball MC, Engelbrecht BM, Ewe ML. Differences in plant function in phosphorus-and nitrogen-limited mangrove ecosystems. New Phytologist 2006; 172(3):514-22.

Marton JM, Herbert ER, Craft CB. Effects of salinity on denitrification and greenhouse gas production from laboratory-incubated tidal forest soils. Wetlands 2012;32: 347-57.

Matus FJ. Fine silt and clay content is the main factor defining maximal C and N accumulations in soils: A meta-analysis. Scientific Reports 2021;11(1):Article No. 6438.

Montzka SA, Dlugokencky EJ, Butler JH. Non-CO_2 greenhouse gases and climate change. Nature. 2011;476(7358):43-50.

Mulya MB, Arlen HJ. Production of litter and detritus related to the density of mangrove. Proceeding of the International Conference on Biological Sciences and Biotechnology (ICBSB); 2018 March 1; Grandhika Setiabudi Medan Hotel, North Sumatra: Indonesia; 2018.

Nazir R, Zaffar R. Climate change extenuation by greenhouse gas quenching microflora. In: Lone SA, Malik A, editors. Microbiomes and the Global Climate Change. Singapore: Springer Nature; 2021. p. 23-41.

Padhy SR, Bhattacharyya P, Dash PK, Reddy CS, Chakraborty A, Pathak H. Seasonal fluctuation in three mode of greenhouse gases emission in relation to soil labile carbon pools in degraded mangrove, Sundarban, India. Science of the Total Environment 2020;705:Article No. 135909.

Perie C, Ouimet R. Organic carbon, organic matter and bulk density relationships in boreal forest soils. Canadian Journal of Soil Science 2008;88(3):315-25.

Prasad MBK, Dittmar T, Ramanathan AL. Organic matter and mangrove productivity. In: Ramanathan AL, Bhattacharya P, Dittmar T, Prasad MBK, Neupane BR, editors. Management and Sustainable Development of Coastal Zone Environments. Netherlands: Springer Nature; 2010. p. 175-93.

Prinasti NK, Dharma IG, Suteja Y. Community structure of mangrove vegetation based on substrate characteristic in Ngurah Rai Forest Park, Bali. Journal of Marine and Aquatic Sciences 2020;6(1):90-9.

Queiroz HM, Artur AG, Taniguchi CA, da Silveira MR, do Nascimento JC, Nobrega GN, et al. Hidden contribution of shrimp farming effluents to greenhouse gas emissions from mangrove soils. Estuarine, Coastal and Shelf Science 2019;221:8-14.

Raganas AF, Magcale-Macandog DB. Physicochemical factors influencing zonation patterns, niche width and tolerances of dominant mangroves in Southern Oriental Mindoro, Philippines. Indo Pacific Journal of Ocean Life 2020;4(2):51-62.

Reay DS, Smith P, Christensen TR, James RH, Clark H. Methane and global environmental change. Annual Review of Environment and Resources 2018;43:165-92.

Robertson GP, Groffman PM. Nitrogen transformations. In: Paul EA, Frey SD, editors. Soil Microbiology, Ecology and Biochemistry. USA: Elsevier; 2024. p. 407-38.

Romero-Uribe HM, López-Portillo J, Reverchon F, Hernández ME. Effect of degradation of a black mangrove forest on seasonal greenhouse gas emissions. Environmental Science and Pollution Research 2022;29:11951-65.

Sidik F, Adame FM, Lovelock CE. Carbon sequestration and fluxes of restored mangroves in abandoned aquaculture ponds. Journal of the Indian Ocean Region 2019;15(2):177-92.

Srikanth S, Lum SK, Chen Z. Mangrove root: Adaptations and ecological importance. Trees 2016;30:451-65.

Sugiana IP, Andiani AAE, Dewi IGAIP, Karang IWGA, As-Syakur AR, Dharmawan IWE. Spatial distribution of mangrove health index on three genera dominated zones in Benoa Bay, Bali, Indonesia. Biodiversitas Journal of Biological Diversity 2022;23(7):3407-18.

Sugiana IP, Faiqoh E, Adame MF, Indrawan GS, Andiani AA, Dewi IG, et al. Soil greenhouse gas fluxes to the atmosphere during the wet season across mangrove zones in Benoa Bay, Indonesia. Asian Journal of Atmospheric Environment 2023;17(13):1-12.

Sugiana IP, Faiqoh E, Indrawan GS, Dharmawan IW. Methane concentration on three mangrove zones in Ngurah Rai Forest Park, Bali. Jurnal Ilmu Lingkungan 2021;19(2):422-31.

Sugiana IP, Prartono T, Rastina, Koropitan AF. Ecosystem carbon stock and annual sequestration rate from three genera-dominated mangrove zones in Benoa Bay, Bali, Indonesia. Biodiversitas 2024;25(1):287-99.

Treat CC, Natali SM, Ernakovich J, Iversen CM, Lupascu M, McGuire AD, et al. A pan-Arctic synthesis of CH_4 and CO_2 production from anoxic soil incubations. Global Change Biology 2015;21(7):2787-803.

Ulumuddin YI. Methane: Greenhouse gas emissions from blue carbon ecosystems, mangroves. Jurnal Ilmu Lingkungan 2018;17(2):359-72.

Ussiri D, Lal R. Formation and release of nitrous oxide from terrestrial and aquatic ecosystems. In: Ussiri D, Lal R, editors. Soil Emission of Nitrous Oxide and Its Mitigation. Netherlands: Springer Nature; 2013. p. 63-96.

Wang D, Chen Z, Sun W, Hu B, Xu S. Methane and nitrous oxide concentration and emission flux of Yangtze Delta plain river net. Science in China Series B: Chemistry 2009;52(5): 652-61.

Weiss C, Weiss J, Boy J, Iskandar I, Mikutta R, Guggenberger G. Soil organic carbon stocks in estuarine and marine mangrove ecosystems are driven by nutrient colimitation of P and N. Ecology and Evolution 2016;6(14):5043-56.

Welti N, Hayes M, Lockington D. Seasonal nitrous oxide and methane emissions across a subtropical estuarine salinity gradient. Biogeochemistry 2017;132:55-69.

Xiong Y, Liu X, Guan W, Liao B, Chen Y, Li M, et al. Fine root functional group-based estimates of fine root production and turnover rate in natural mangrove forests. Plant and Soil 2017;413:83-95.

Xu Y, Liao B, Jiang Z, Xin K, Xiong Y, Guan W. Emission of greenhouse gases (CH_4 and CO_2) into the atmosphere from restored mangrove soil in South China. Journal of Coastal Research 2021;37(1):52-8.

Yost JL, Hartemink AE. Soil organic carbon in sandy soils: A review. Advances in Agronomy 2019;158:217-310.

Zhu X, Burger M, Doane TA, Horwath WR. Ammonia oxidation pathways and nitrifier denitrification are significant sources of N_2O and NO under low oxygen availability. Proceedings of the National Academy of Sciences 2013;110(16):6328-33.

Zumft WG, Kroneck PM. Respiratory transformation of nitrous oxide (N_2O) to dinitrogen by bacteria and archaea. Advances in Microbial Physiology 2006;52:107-227.